the cancers are identified. Examples include gefitinib for EGFR mutation-positive lung adenocarcinoma and crizotinib for EML4-ALK positive lung adenocarcinoma.

With regard to these advances in molecular phenotyping, identification of particular histopathological subtypes of lung adenocarcinomas, including bronchioloalveolar pattern or mucinous cribriform pattern, will give important clues for therapeutically tractable genomic changes, such as EGFR gene mutations or EML4-ALK fusion gene.

Reported herein is a case of synchronous EML4-ALK positive lung adenocarcinoma and adenocarcinoma in situ in the bilateral lungs of a 55-year-old Japanese woman. The woman had EML4-ALK positive lung adenocarcinoma in the right lower lung while adenocarcinoma in situ in the left upper lung.

Case presentation

A 55-year-old Japanese woman was referred to Yodogawa Christian Hospital because of incidental finding of an abnormal shadow in the chest X-ray. She was a never-smoker. Chest computerized tomography (CT) examination revealed a 38×12mm-sized stellate-shaped mass in the right lower lobe (Figure 1a) and a 15×10mm ground-glass opacity shadow in the left upper lobe of the lung (Figure 1b). Apparently no enlargement of mediastinal lymph nodes were detected on the CT. Endoscopic biopsy of the left lung tumor showed adenocarcinoma (data not shown). Right lower lobectomy and left upper segmentectomy were performed to resect both mass. Cut surface of the resected tumors revealed a gray stellate-shaped mass in the right lung and a white and yellowish mass with relatively clear border in the left lung (data not shown).

Figure 1 Preoperative chest CT image reveals a 38×12mm stellate-shaped mass in the right lower lobe (a) and a 15×10mm ground-glass opacity shadow in the left upper lobe of the lung (b).

The tissue was fixed in 10% buffered formalin and embedded in paraffin. Three-micrometer-thick sections were stained with hematoxylin and eosin (HE). Immunohistochemistry was performed on representative sections with appropriate antigen retrieval. A primary antibody against ALK was purchased from NICHIREI (NICHIREI 413681; clone #5A4) and the immunostained signal was visualized using I-VIEW DAB universal kit (Roche diagnostics, Switzerland). For mutational analysis, genomic DNA was extracted from formalin-fixed, paraffin-embedded tissue sections using Genomic DNA Extraction Kit (Qiagen, Hilden, Germany). DNA sequencing for EGFR gene mutation was performed as described [10] with minor modifications. Fluorescent in situ hybridization (FISH) analysis using probes for EML4 and ALK genes was performed as described previously [7].

Microscopic examination of the resected right lower lobe revealed a heterogenous adenocarcinoma composed of a mucinous cribriform tumor (Figure 2a) and lepidic growth (adenocarcinoma in situ) pattern (Figure 2c). At low-power microscopy, these two components were seen adjacent to each other (data not shown). As described above, the mucinous cribriform histology of the HE stained specimen made us suspicious of EML4-ALK positive lung adenocarcinoma [5-7]. To examine this possibility, immunohistochemical analysis was performed. At low-power microscopy, the tumor was homogeneously stained positive for ALK (data not shown). At high-power microscopy, the tumor cells were

positively stained for ALK (Figures 2b,d). Fusion and split FISH analyses using probes for EML4 and ALK genes confirmed that the adenocarcinoma of the right lung was indeed EML4-ALK positive (Figures 2g-j). We confirmed that the EML4-ALK positive adenocarcinoma has no mutations in exons 18, 19, 20, 21 of EGFR gene (data not shown).

Figure 2 Histological and FISH analysis. Microscopic and immunohistochemical examination of the right lung cancer reveals a mucinous cribriform pattern (**a**) (HE stain, ×200), which is positive for ALK (**b**) (immunohistochemical staining, ×200). The right lung cancer also contains a bronchioloalveolar pattern (**c**) (HE stain, ×200), which is again positive for ALK (**d**) (immunohistochemical staining, ×200). On the other hand, the left lung cancer is composed singly of a bronchioloalveolar pattern (**e**) (HE stain, ×200), which is negative for ALK (**f**) (immunohistochemical staining, ×200). FISH analyses revealed EML4-ALK fusion gene in the tumor of the right lung (**g-j**). FISH signals in a single tumor cell are shown. (**g**)-(**i**) EML4-ALK fusion FISH. The signals for ALK gene (**g**) and EML4 gene (**h**) are indicated by green and red dots, respectively. The signal for EML4-ALK fusion gene is indicated by a white arrow (**i**). (**j**) ALK split FISH. The signals for 5′ and 3′ probe for ALK gene are indicated by green and red dots, respectively. Split of the green and the red dots is consistent with the presence of EML4-ALK fusion gene.

On the other hand, the resected left upper lobe specimen contained a adenocarcinoma in situ (Figure 2e). This tumor was negative for ALK (Figure 2f). We searched for EGFR mutations for exons 18, 19, 20, and 21 in the genomic DNA from the adenocarcinoma in situ, but none of them were found (data not shown).

As an adjuvant therapy, the patient has taken orally tegafur-uracil 300 mg/day since 3 months after the resection operation. Until now, she has not shown any signs of relapse or adverse effects. Eleven months after the operation, neither chest CT, nor bone scintigraphy, nor brain magnetic resonance imaging did show any signs of relapse or metastasis.

Conclusion

In this report, we described a case of synchronous bilateral lung cancers with EML4-ALK positive adenocarcinoma in the right lung and adenocarcinoma in situ in the left, which was EML4-ALK negative. To our knowledge, this is the first report of a case of synchronous lung adenocarcinomas of this combination.

A number of cases of synchronous multiple lung adenocarcinomas were reported previously. The most frequent components in those cases were well differentiated adenocarcinoma with mixed bronchioloalveolar pattern [11]. Graziano et al. [12] reported a case of synchronous bilateral adenocarcinoma in situ of the lung with distinct mutations of EGFR gene. Some of these cases were associated with atypical adenomatous hyperplasia [13,14]. Adenocarcinoma in situ of the lung was frequently associated with EGFR gene mutation [15,16]. There is a case of multiple adenocarcinomas in situ of the lung having the same mutation of EGFR in common [17].

In our case, although the bilateral adenocarcinomas have bronchioloalveolar pattern in common, the right lung cancer was EML4-ALK positive while the left one was not. Furthermore, EGFR gene mutations were not detected in the exons 18 to 21 in "pure" bronchioloalveolar adenocarcinoma in the left lung. Over 90% of EGFR mutations were

reported to be localized in these 4 exons [18]. Thus, it is unlikely that the adenocarcinoma in situ in the left lung has EGFR mutation. Interestingly, Togashi et al. recently identified KLC1-ALK fusion gene in a case of adenocarcinoma in situ of the lung [19]. However, in our case, the adenocarcinoma in situ of the left lung was immunohistochemically negative for ALK. Therefore, it is unlikely that the left lung cancer is ALK fusion-positive. The right tumor and the left one had lepidic growth pattern in common, although the former was EML4-ALK positive, while the latter negative. The relationship between genetic alterations and histology is intriguing and it will be interesting to compare gene expression profiling of both tumors.

The fact that the tumor of the right lung and that of the left lung harbor different genetic alterations will be useful for the follow-up of this patient. The adenocarcinoma in situ of the left lung was 15x10mm of size and pathologically at stage 0 (TisN0M0). Therefore, the possibility of presenting metastasis in the following five years is as low as nearly 0%. On the other hand, the EML4-ALK-positive tumor of the right lung was an invasive cancer. Thus, if any metastasis or relapse occurs in the future in this patient, it is more likely that the relapse derives from EML4-ALK-positive cancer of the right lung. After the confirmation that the metastasis or relapse harbor EML4-ALK translocation, ALK inhibitor such as crizotinib will be the first choice. EML4-ALK fusion gene occurred around 3% of "non-smoker" adenocarcinomas of the lung [7]. In addition to the EML4-ALK fusion, not only other fusion partner for ALK gene, but also novel kinase gene fusions have been discovered in a subset of lung adenocarcinoma [7-9]. It was reported that these kinase gene fusion-positive lung adenocarcinomas have some histological correlates or surrogates including mucinous cribriform pattern [7]. However, as our case report illustrated, kinase gene fusion-positive lung adenocarcinomas may show different histology other than mucinous cribriform pattern. Not only tumor histology, but also patients' sex, age, smoking habit, and so on, should be considered to suspect the involvement of kinase gene fusion in lung cancers. Although rarer than lung cancer with EGFR mutation, the identification of kinase gene fusions, including EML4-ALK, in lung cancer leads to molecularly-targeted therapy with kinase inhibitors. The identification has important implication for tractable therapy and predictable prognosis.

Consent

Written informed consent was obtained from the patient for publication of this Case report and any accompanying images. A copy of the written informed consent is available for review by the Editor-in-Chief of this journal.

Abbreviations

EGFR, Epidermal growth factor receptor; EML4, Echinoderm microtubule-associated protein like 4; ALK, Anaplastic large cell lymphoma kinase; CT, Computerized tomography; HE, Hematoxylin and eosin; FISH, Fluorescent in situ hybridization

Competing interests

All the authors state no competing interests.

Authors' contribution

IM, Kengo Takeuchi, KU, Kazuhiro Teramura, and SH participated in the pathological final diagnosis of the case, and prepared and edited the manuscript. In particular, Kengo Takeuchi performed the FISH analysis. SM and MK were responsible for the preoperative endoscopic examination and the operations, and helped IM and SH in preparation of the manuscript. All authors read and approved the final manuscript.

References

1. Travis WD, Brambilla E, Muller-Hermelink HK, Haris CC, World Health Organization: *Classification of Tumours. Pathology & Genetics: tumours of the lung, pleura, thymus, and heart.* Lyon: IARC Press; 2004.

2. Travis WD, Brambilla E, Noguchi M, Nicholson AG, Geisinger KR, Yatabe Y, Beer DG, Powell CA, Riely GJ, Van Schil PE, *et al*: **International association for the study of lung cancer/american thoracic society/european respiratory society international multidisciplinary classification of lung adenocarcinoma.** *J Thorac Oncol* 2011, **6**:244–285.

3. Ding L, Getz G, Wheeler DA, Mardis ER, McLellan MD, Cibulskis K, Sougnez C, Greulich H, Muzny DM, Morgan MB, *et al*: **Somatic mutations affect key pathways in lung adenocarcinoma.** *Nature* 2008, **455**:1069–1075.

4. Soda M, Choi YL, Enomoto M, Takada S, Yamashita Y, Ishikawa S, Fujiwara S, Watanabe H, Kurashina K, Hatanaka H, *et al*: **Identification of the transforming EML4-ALK fusion gene in non-small-cell lung cancer.** *Nature* 2007, **448**:561–566.

5. Inamura K, Takeuchi K, Togashi Y, Nomura K, Ninomiya H, Okui M, Satoh Y, Okumura S, Nakagawa K, Soda M, *et al*: **EML4-ALK fusion is linked to histological characteristics in a subset of lung cancers.** *J Thorac Oncol* 2008, **3**:13–17.

6. Inamura K, Takeuchi K, Togashi Y, Hatano S, Ninomiya H, Motoi N, Mun MY, Sakao Y, Okumura S, Nakagawa K, *et al*: **EML4-ALK lung cancers are characterized by rare other mutations, a TTF-1 cell lineage, an acinar histology, and young onset.** *Mod Pathol* 2009, **22**:508–515.

7. Takeuchi K, Soda M, Togashi Y, Suzuki R, Sakata S, Hatano S, Asaka R, Hamanaka W, Ninomiya H, Uehara H, *et al*: **RET, ROS1 and ALK fusions in lung cancer.** *Nat Med* 2012, **18**:378–381.

8. Kohno T, Ichikawa H, Totoki Y, Yasuda K, Hiramoto M, Nammo T, Sakamoto H, Tsuta K, Furuta K, Shimada Y, *et al*: **KIF5B-RET fusions in lung adenocarcinoma.** *Nat Med* 2012, **18**:375–377.

9. Ju YS, Lee WC, Shin JY, Lee S, Bleazard T, Won JK, Kim YT, Kim JI, Kang JH, Seo JS: **A transforming KIF5B and RET gene fusion in lung adenocarcinoma revealed from whole-genome and transcriptome sequencing.** *Genome Res* 2012, **22**:436–445.

10. Paez JG, Jänne PA, Lee JC, Tracy S, Greulich H, Gabriel S, Herman P, Kaye FJ, Lindeman N, Boggon TJ, *et al*: **EGFR mutations in lung cancer: correlation with clinical response to gefitinib therapy.** *Science* 2004, **304**:1497–1500.

11. Nakata M, Sawada S, Yamashita M, Saeki H, Kurita A, Takashima S, Tanemoto K: **Surgical treatments for multiple primary adenocarcinoma of the lung.** *Ann Thorac Surg* 2004, **78**:1194–1199.

12. Graziano P, Cardillo G, Mancuso A, Paone G, Gasbarra R, De Marinis F, Leone A: **Long-term disease-free survival of a patient with synchronous bilateral lung adenocarcinoma displaying different EGFR and C-MYC molecular characteristics.** *Chest* 2011, **140**:1354–1356.

13. Dohmoto K, Fujita J, Ohtsuki Y, Kotsuna N, Mitsunaka H, Kuwabara H, Takahara J: **Synchronous four primary lung adenocarcinoma associated with multiple atypical adenomatous hyperplasia.** *Lung Cancer* 2000, **27**:125–130.

14. Suzuki K, Takahashi K, Yoshida J, Nishimura M, Yokose T, Nishiwaki Y, Nagai K: **Synchronous double primary lung carcinomas associated with multiple atypical adenomatous hyperplasia.** *Lung Cancer* 1998, **19**:131–139.

15. Miller VA, Kris MG, Shah N, Patel J, Azzoli C, Gomez J, Krug LM, Pao W, Rizvi N, Pizzo B, *et al*: **Bronchioloalveolar pathologic subtype and smoking history predict sensitivity to gefitinib in advanced non-small-cell lung cancer.** *J Clin Oncol* 2004, **22**:1103–1109.

16. Yatabe Y, Kosaka T, Takahashi T, Mitsudomi T: **EGFR mutation is specific for terminal respiratory unit type adenocarcinoma.** *Am J Surg Pathol* 2005, **29**:633–639.

17. Yoshimoto K, Yoshida J, Ishii G, Nishimura M, Hishida T, Nagai K: **Two lung adenocarcinomas in the same lobe: multiple primaries or intrapulmonary metastasis?** *Ann Thorac Cardiovasc Surg* 2011, **17**:584–587.

18. Mitsudomi T, Yatabe Y: **Mutations of the epidermal growth factor receptor gene and related genes as determinants of epidermal growth factor receptor tyrosine kinase inhibitors sensitivity in lung cancer.** *Cancer Sci* 2007, **98**:1817–1824.

19. Togashi Y, Soda M, Sakata S, Sugawara E, Hatano S, Asaka R, Nakajima T, Mano H, Takeuchi K: **KLC1-ALK: a novel fusion in lung cancer identified using a formalin-fixed paraffin-embedded tissue only.** *PLoS One* 2012, **7**:e31323.

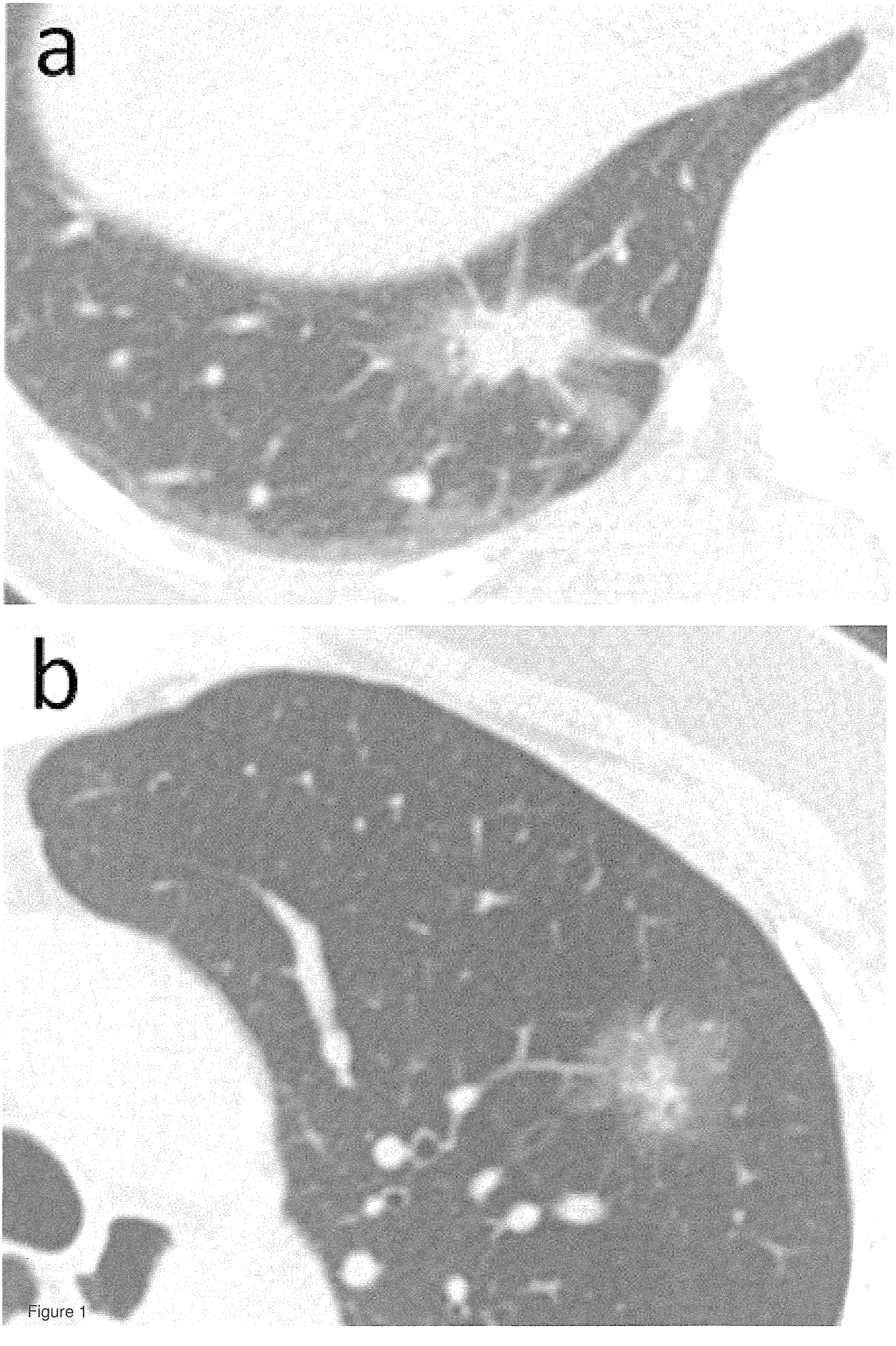

Figure 1

a
b
c
d
e
f
g
h
i
j

Diagnostic Pathology

BioMed Central
The Open Access Publisher

Inflammatory myofibroblastic tumor with RANBP2 and ALK gene rearrangement: a report of two cases and literature review

Diagnostic Pathology 2013, **8**:147 doi:10.1186/1746-1596-8-147

Jian Li (lijianhouma@yahoo.cn)
Wei-hua Yin (weihuayin@sina.com)
Kengo Takeuchi (kentakeuchi-tky@umin.net)
Hong Guan (hongguansz@sina.cn)
Yu-hua Huang (yuhuahuang@yahoo.cn)
John KC Chan (jkcchan@ha.org.hk)

ISSN 1746-1596

Article type Case Report

Submission date 31 May 2013

Acceptance date 5 August 2013

Publication date 13 September 2013

Article URL http://www.diagnosticpathology.org/content/8/1/147

Inflammatory myofibroblastic tumor with *RANBP2* and *ALK* gene rearrangement: a report of two cases and literature review

Jian Li[1]
Email: lijianhouma@yahoo.cn

Wei-hua Yin[1]
Email: weihuayin@sina.com

Kengo Takeuchi[2,3]
Email: kentakeuchi-tky@umin.net

Hong Guan[4*]
[*] Corresponding author
Email: hongguansz@sina.cn

Yu-hua Huang[4]
Email: yuhuahuang@yahoo.cn

John KC Chan[5]
Email: jkcchan@ha.org.hk

[1] Department of Pathology, Peking University Shenzhen Hospital, No. 1120, Lianhua North Road, Shenzhen 518000, China

[2] Pathology Project for Molecular Targets of the Cancer Institute, Tokyo 135-8550, Japan

[3] Division of Pathology of the Cancer Institute Hospital, Japanese Foundation for Cancer Research, 3-8-31 Ariake, Koto, Tokyo 135-8550, Japan

[4] Department of Pathology, the Second Shenzhen People's Hospital, Sungang West Road, Shenzhen 518035, China

[5] Department of Pathology, Queen Elizabeth Hospital, Hong Kong, SAR, China

Abstract

Inflammatory myofibroblastic tumors (IMTs) are categorized as intermediate biologic neoplasms, whereas IMTs with genetic features of ran-binding protein 2 (*RANBP2*) and anaplastic lymphoma kinase (*ALK*) rearrangement (IMT-RAs) are possibly related to a more aggressive clinical course. However, fewer than 10 cases of IMT-RA have been reported to date. Herein, we present 2 new cases of IMT-RA in which both tumors recurred quickly after primary surgery; one patient died 3 months later from the disease, and the other patient has been living with the disease for 12 months. IMT-RAs are characterized by noncohesive epithelioid and rounded tumoral cell morphology, commonly derived from pelvic and

peritoneal cavities, and frequently show larger tumor sizes. The relation between the clinicopathologic features and poor prognosis of IMT-RA is discussed.

Virtual slides

http://www.diagnosticpathology.diagnomx.eu/vs/3314123381007714

Keywords

Inflammatory myofibroblastic tumor, RANBP2-ALK, Fluorescence in situ hybridization

Background

Inflammatory myofibroblastic tumors (IMTs) are mesenchymal neoplasms of intermediate biologic potential that are derived from myofibroblastic cells and accompanied by rich inflammatory infiltrates [1]. IMTs have a predilection for children and adolescents, and the most common anatomical locations are the abdominopelvic region, lung, and retroperitoneum. IMTs show expression of anaplastic lymphoma kinase (ALK) protein triggered by *ALK* gene (at 2p23) rearrangement, which has been found in 36–60% of IMTs [2]. ALK fusion oncogenes have been identified in a small proportion of IMTs, including *SEC31L1* at 4q21, *ATIC* at 2q35, *CARS* at 11p15, *TPM3* at 1p23, *TMP4* at 19p13, *CLTC* at 17q23, *PPFIBP1* at 12p11, and ran-binding protein 2 (*RANBP2*) at 2q13 [3]. Different fusion partners may lead to distinct subcellular locations of the corresponding chimeric protein, which result in distinct immunostaining patterns when detected by ALK antibody. IMTs with CARS, ATIC, and SEC31L1 fusion are generally associated with smooth cytoplasmic staining, whereas fusion with CLTC, a main structural protein of coated vesicles, displays a granular cytoplasmic pattern [4].

RANBP2 fuses with the *ALK* gene through balanced or unbalanced translocation [5]. The *RANBP2* gene encodes a 358-kd nuclear pore protein [6], thus IMTs with *RANBP2-ALK* (IMT-RA) rearrangement display a unique nuclear membrane staining pattern. Most importantly, IMT-RA is possibly associated with a poor prognosis; however, this relation remains inconclusive, as fewer than 10 cases of IMTs with genetically confirmed *RANBP2-ALK* fusion have been reported to date [5,7-11]. Herein, we present 2 new cases of IMT-RA with follow-up information. The relations between the histopathologic features and prognosis of IMT-RAs are discussed further.

Case presentation

Case 1 was a 19-year-old female who was hospitalized due to paroxysmal abdominal pain combined with nausea and vomiting for 4 days. Ultrasound examination showed a 19 × 17 × 11 cm solid mass in the pelvic cavity and medium amounts of ascitic fluid. Intraoperatively, the tumor was situated in the mesenterium region of the terminal ileum, and had locally invaded into the adjacent ileum wall. Resections of the tumor, affected terminal ileum, and ileocecum were performed. The patient rejected further chemotherapy. Nine weeks after the operation, radiological imaging displayed recurrent intra-abdominal occupations with massive ascites. Concurrently, acute renal insufficiency was identified by laboratory tests. The patient died of the disease after 3 weeks of maintenance treatment.

Case 2 was a 39-year-old male with an initial complaint of laborious urination for more than 2 months and abdominal distention and abdominal pain for 10 days. Computer Tomography (CT) revealed a 15 × 10 × 8 cm occupation in the pelvic cavity (Figure 1). The neoplasm was found in the mesangial region at the junction of sigmoid and rectum during the operation, with invasions of the neighboring sigmoid, the upper portion of the rectum, and left ureter. The tumor and afflicted intestines and left ureter were completely excised. The patient was treated with epirubicin and iphosphamide following the operation. Four months after the first excision, CT showed multiple recurrent masses in the presacral, pararectal, and left iliac vessel regions. The patient then underwent chemoembolization therapy. Follow-up has continued to date, and the patient has lived with the tumor for 12 months.

Figure 1 Computer tomography of Case 2 revealed a heterogeneous-density occupation in the left pelvic cavity.

Histopathological and genetic findings

The gross and histological features were similar in Case 1 and Case 2. The tumors were solid and gray-yellowish in the cut surface. Focal hemorrhage and a myxomatous appearance were observed. Microscopically, the neoplasm showed a fasciitis-like pattern and the stromal myxoid change was prominent (Figure 2A, B). The tumor cells were generally non-cohesive, and frequently demonstrated ganglion-like morphology of slightly amphophilic cytoplasm, vesicular chromatin, and large nucleoli (Figure 2C). There were also a few binucleate cells sparsely presented in the lesion (Figure 2D). In area of the neoplasm, some tumor cells were tightly packed and arranged in sheets (Figure 2E). The mitotic figures ranged from 1 to 4 per 10 high-power fields. There were abundant admixed polymorphs infiltrates, including neutrophils, eosinophils, and lymphoplasma cells, which were unevenly distributed throughout the lesion. Erythrocyte extravasation was another feature found in both cases. The tumor invaded the adjacent intestinal tissues, involving the adventitia, muscularis propria, and submucosa with a vague nodular pattern (Figure 2F).

Figure 2 Histopathological findings of inflammatory myofibroblastic tumor with *RANBP2* and *ALK* gene rearrangement. (A) and **(B)** The neoplastic cells were loosely arrayed and distributed in an abundant myxoid stroma. There were striking neutrophilic inflammatory infiltrates in the lesion, while lymphoplasma cells were only occasionally observed (inserted panel) (A and B, hematoxylin and eosin [H&E] staining, 200× original magnification; inserted panel, H&E staining, 400× original magnification). **(C)** The tumor cells showed ganglion-like morphology, characterized by an abundant and slightly amphophilic cytoplasm, round nuclei, vesicular chromatin, and large nucleoli (H&E staining, 400× original magnification). **(D)** A few binucleate cells were found in the tumor (H&E staining, 400× original magnification). **(E)** In focal area, the tumor cells were tightly packed around dilated vessels (H&E staining, 100× original magnification). **(F)** The tumor infiltrated the adjacent intestinal wall in a vague nodular pattern (H&E staining, 40× original magnification).

Immunohistochemically, the tumor cells showed distinctive nuclear membrane staining for ALK (Dako; Clone ALK1; Ready-to-use) (Figure 3A) in both cases. Similarly, positive staining for CD30 (Dako; Clone Ber-H2; 1:40 dilution) (Figure 3B), desmin (Dako; Clone D33; 1:100 dilution) (Figure 3C), and SMA (Dako; Clone 1A4; 1:100 dilution) was also observed in some tumor cells in the 2 cases. In both cases, the tumor cells were nonreactive to AE1/AE3 (Dako; Clone AE1 + AE3; 1:200 dilution), cytokeratin 8/18 (Santa Cruz

Biotechnology; Clone NCL-5D3; 1:100 dilution), CD117 (Dako; polyclonal; 1:100 dilution), calponin (Santa Cruz Biotechnology; Clone CALP; 1:200 dilution), S100 (Dako; polyclonal; 1:500 dilution), CD21 (Dako; Clone 1 F8; 1:25 dilution), HMB45 (Dako; 1:50 dilution), myogenin (Dako; Clone F5D; 1:50 dilution), and Myf4 (Novocastra; Clone LO26; 1:500 dilution).

Figure 3 Immunohistochemistry features of inflammatory myofibroblastic tumor. The tumor cells showed nuclear membranous ALK immunostaining **(A)**, cytomembranous CD30 immunostaining **(B)**, and cytoplasmic desmin immunostaining **(C)** (A and B, 400× original magnification; C, 200× original magnification). **(D)** Interphase fluorescence *in situ* hybridization (FISH) revealed 1 fused signal (arrow) in the tumor nucleus, indicating the presence of *RANBP2-ALK* translocation. One separate orange signal and 1 separate green signal indicated a normal *ALK* and a normal *RANBP2* locus, respectively (1000× original magnification).

Fluorescence *in situ* hybridization (FISH) was performed on 4 μm-thick tissue sections with bacterial artificial chromosome probes for *RANBP2* (RP11-348G16) and *ALK* (RP11-984I21 and RP11-62B19). In both cases, 1 fused signal was observed in the tumor cell nucleus, indicating the presence of *RANBP2* and *ALK* gene rearrangement (Figure 3D) by unbalanced genetic rearrangement mechanism [5].

To pinpoint the fusion location of the *RANBP2* and *ALK* genes, reverse-transcription polymerase chain reaction (RT-PCR) analysis was performed. Total RNA was extracted from 15 μm-thick paraffin sections using the RNeasy® FFPE kit (QIAGEN, Germany), and reverse-transcribed using random hexamer primers. PCR was performed using previously introduced primers [8] for 45 cycles as follows: 94°C for 30 seconds, 60°C for 30 seconds, and 72°C for 30 seconds. An expected 254-bp amplification product was detected in Case 2 (Figure 4A). No PCR product was identified in Case 1, which may be due to RNA degradation in the paraffin-embedded block since positive amplification results (285-bp) of beta-actin as a householding gene were not found either in Case 1 but present in Case 2 (Figure 4B). Direct sequencing of the chimeric cDNA product confirmed that the *RANBP2-ALK* fusion point was composed of exon 18 of *RANBP2* to exon 20 of *ALK* (Figure 4C).

Figure 4 Genetic features of inflammatory myofibroblastic tumor. (A) Reverse-transcription polymerase chain reaction (RT-PCR) with *RANBP2* and *ALK* primers. Lane T1: no amplification band was observed in Case 1. Lane T2: an expected 254-bp product was present in Case 2. Lane C: tonsil tissue was adopted as a control, and no amplification band was observed. Lane NTC: no template control. **(B)** Detection of house-keeping gene of beta-actin by RT-PCR. An expected 285-bp product was seen in Case 2 (Lane 2) and tonsil tissue (Lane 3). No amplification band was observed in Case 1 (Lane 1) and no-template control (Lane NTC). **(C)** The fusion point of the *RANBP2-ALK* gene as indicated by cDNA sequencing was located between exon 18 of the *RANBP2* gene and exon 20 of the *ALK* gene.

Discussion

IMT is regarded as a neoplasm of intermediate biologic potential. Overall, the recurrence rate varies by anatomical sites, from 2% for tumors confined to the lung to 25% for extrapulmonary lesions. Distant metastasis of IMT occurs in less than 5% of cases [12]. According to the literature and the 2 cases presented herein (Table 1), the local recurrence

rate of IMT-RA is 88% (7/8) with a metastasis rate of 25% (2/8), both markedly higher than those of conventional IMTs. Furthermore, 2 patients (25%, 2/8) have died from the disease within 6 months after the tumor excision. These data suggest that IMT-RAs are more invasive clinically.

Table 1 Clinical features of 11 cases of inflammatory myofibroblastic tumor with *RANBP2-ALK* gene fusion

Case	Author	Age	Sex	Anatomic site(s)	Size (cm)	Treatment	Follow-up
1	Ma [5] (2003)	7 y	Male	Unspecified abdominal mass	NA	SE + CT	Recurred 5 weeks later after first resection. A re-excision was performed. Five months later, the tumor recurred again and was re-excised.
2		7 m	Male	Mesentery and omentum	11	SE	Recurred 8 months later after first resection. A re-excision was performed.
3	Patel [7] (2007)	2 y	Male	Retroperitoneal abdominal mass	10	SE	No evidence of recurrence with 3 years of follow-up.
4	Chen [8] (2008)	34 y	Male	Liver	8	SE	Recurred 5 months later after resection. Died of the disease approximately 2 weeks after discovery of the recurrence.
5	Butrynski [9](2010)	44 y	Male	Omentum	NA	SE + CT + ALKi	Hepatic, peripancreatic, and perirectal masses recurred 1 year later after resection. Subsequent exploratory laparotomy with maximal debulking was performed.
6	Marino-Enriquez [10] (2011)	41 y	Male	Omentum	26	SE + CT + ALKi	Multifocal local recurrence and liver metastases. Alive with no evidence of disease for 40 months.
7		6 y	Male	Omentum and Mesentery	14	SE	NA
8		39 y	Male	Mesentery of the small bowel	14	SE	NA
9	Kozu [11] (2013)	57 y	Male	Pluera or chest wall	NA	ALKi	NA
10	Present cases (2013)	19 y	Female	Mesentery of the small bowel	19	SE	Recurred 9 weeks later after resection. Died of the disease 3 weeks later after discovery of the recurrence.
11		39 y	Male	Mesentery of the colon	15	SE + CT	Recurred 4 months later after resection. Alive with disease for 12 months.

SE: surgical excision; CT: chemotherapy; ALKi: ALK inhibitor; NA: data not available.

The aggressive behavior of IMT-RA might be associated with the following aspects: (1) The location and size of the tumor: Coffin et al. [13] analyzed the clinicopathologic features of IMTs with an invasive course, and found that IMTs that arise in the abdominopelvic site are more likely to recur (with a recurrence rate of 85%). In addition, recurrent and metastatic IMTs were commonly larger in size, with mean diameters of 8.7 and 11 cm, respectively. Of the 11 reported cases of IMT-RAs, 10 occurred in the abdominopelvic area, and only 1 presented in the pleural cavity (no follow-up data were provided in the case). The average size on discovery was 14.6 cm. Thus, the aggressiveness of IMT-RA is possibly related at least in part to its abdominopelvic origination and bigger tumor size. It is worth noting that IMT-RA seemingly prefers to afflict male patients, as the male to female ratio is 10:1.

(2) The histological features of the tumor: The morphology of IMT-RAs is generally uniform and characterized by loosely arrayed, ganglion-like or epithelioid neoplastic cells distributed in a widespread myxoid stroma. In earlier reports, IMTs with the aforementioned features were named round cell transformation [14]. It has been well demonstrated that IMTs with round cell transformation behave aggressively with rapid recurrence and/or death, compared to conventional IMTs in which spindled tumoral cells predominate [14]. Marino-Enriquez [10] proposed to designate this type of IMT as epithelioid inflammatory myofibroblastic sarcoma based on its histological and malignant biological characteristics. Therefore, the distinctive histology of IMT-RAs dominated by epithilioid neoplastic cells also intrinsically reflects the heightened invasiveness of the tumor. However, it should be particularly noted that not all IMTs with round cell morphology carry the genetic alteration of IMT-RA [8]. Therefore, it is inappropriate to diagnosis IMT-RA based solely on morphologic features.

(3) The genetic features of the tumor: The fusion point of IMT-RAs reported to date constantly presents between exon 18 of *RANPB2* and exon 20 of *ALK*. (Table 2) Sasaki [15] found that the *RANPB2-ALK* fusion gene could lead to interleukin (IL)-3 independent growth of Ba/F3 cells. Similarly, another study showed that bone marrow cells transfected with the *RANBP2-ALK* gene acquired an enhanced colony-forming potential and a decreased dependency on cytokine [16]. These studies suggested that the chimeric *RANPB2-ALK* gene could promote cellular proliferation, which might be a potential mechanism for the rapid regrowth and recurrence of IMT-RA. However, there is still a lack of direct experimental evidence linking the functions of this fusion gene with the increased aggressiveness of IMT-RA.

Table 2 Genetic and immunohistochemical characteristics of 11 cases of inflammatory myofibroblastic tumor with *RANBP2-ALK* gene fusion

Case	Genetic features		Immunohistochemical features							
	RANBP2 to *ALK* fusion point	Detection techniques	ALK	desmin	SMA	caldesmin	CD30	CK	EMA	S100
1	Exon 18 to exon 20	RT-PCR, FISH	NM+	/	/	/	/	/	/	/
2	Exon 18 to exon 20	RT-PCR, FISH	NM+	/	/	/	/	/	/	/
3	Exon 19 to exon 20*	RT-PCR, FISH	CP+	+	+	-	/	+	/	-
4	Exon 18 to exon 20	RT-PCR	NM+	-	-	/	-	-	/	-
5	Exon 18 to exon 20	RT-PCR	NM+	+	-	/	/	-	/	/
6	Exon 18 to exon 20	RT-PCR	NM+	+	-	-	+	-	-	-
7	Exon 18 to exon 20	RT-PCR	NM+	+	/	-	+	/	/	-
8	Exon 18 to exon 20	RT-PCR	NM+	+	+	-	+	-	/	-
9	Unknown	FISH	CP+	+	-	/	-	+	/	-
10	Unknown	FISH	NM+	+	+	-	+	-	-	-
11	Exon 18 to exon 20	RT-PCR, FISH	NM+	+	+	-	+	-	-	-
Total	/	/	100% (11/11)	89% (8/9)	50% (4/8)	0% (0/6)	71% (5/7)	25% (2/8)	0% (0/3)	0% (0/8)

NM: nuclear membrane; CP: cytoplasm.

*Reference 7 stated that the fusion point was exon 19 of *RANBP2* to exon 20 of *ALK*, while Figure 2 in the paper indicated that the actual fusion location was exon 18 of *RANBP2* to exon 20 of *ALK*.

From a diagnostic viewpoint, IMT-RA needs to be differentiated from a large group of tumors that manifest epithelioid features. Immunohistochemistry is greatly helpful in this process. Nuclear membrane staining of ALK is a unique immunophenotype of IMT-RA, which is observed in 82% (9/11) of cases. Unexplainably, a cytoplasmic pattern is also detected in 18% (2/11) of cases. In addition, the neoplasms display varied expression of

desmin (89%, 8/9), CD30 (71%, 5/7), SMA (50%, 4/8), and cytokeratin (25%, 2/8), while EMA, S100, CD117, Myf4, myogenin, caldesmin, and HMB45 expression is consistently negative. Therefore, IMT-RAs could be easily distinguished from poorly differentiated carcinoma, malignant melanoma, epithelioid gastrointestinal stromal tumor, epithelioid solitary fibrous tumor [17], myofibroma [18] and alveolar rhabdomyosarcoma. It is noteworthy that a few mesenchymal mimics listed below may also show cytoplasmic ALK staining [19] and thus should particularly be discriminated to avoid misdiagnosis. (1) Epithelioid leiomyosarcoma (ELS): Compared with IMT-RA, ELS commonly displays greater cellular atypia and pleomorphism, and higher cellular density. ELS generally lacks an extensive myxoid background and inflammatory infiltrates. Furthermore, calponin and caldesmin expression could be recognized in ELS but not in IMT-RA [20]. (2) Inflammatory malignant fibrous histiocytoma (IMFH): Clinically, IMFH is more prone to occur in elderly individuals, which is different from IMT-RA that typically develops in young adults (median age, 34 years). Histologically, while the inflammatory infiltrates may be striking in both types of the tumors, the neoplastic cells in IMFH tend to be more pleomorphic, in contrast with the relative homogeneity in cellular morphology of IMT-RA. The neoplastic cells in IMFH are frequently fusiform and closely packed, and commonly arranged in a storiform pattern. Immunostaining of CD68 favors the diagnosis of IMFH. (3) Epithelioid malignant peripheral nerve sheath tumor (E-MPNST): Most E-MPNSTs develop from the setting of neurofibromatosis. E-MPNST presents with more or fewer spindled tumor cells in the lesion, and the myxoid stroma is more often focal rather than abundant [21,22]. Moreover, desmin and CD30 expression have not been discovered in E-MPNSTs. All of these features differ from those of IMT-RA. (4) Anaplastic large cell lymphoma (ALCL): The distinction between IMT-RA and ALCL has been described in a previous report [10]. Desmin and nuclear membrane ALK staining are suggestive of IMT-RA, as neither of these staining patterns has been observed in ALCL.

Most of the reported IMT-RAs are treated by surgical resection combined with chemotherapy. However, this therapeutic regimen seems to not effectively control the rapid recurrence of IMT-RAs. Recently, ALK inhibitor (ALKi) has been applied in the therapy of 2 IMT-RA cases, and a sustained partial response has been observed in at least 1 case [9]. Of note, the sensitivity of ALKi was reduced during standing treatment because of a secondary *ALK* gene mutation [15]. Thus, the long-term results of ALKi therapy remain to be further evaluated.

Conclusions

In comparison with conventional IMTs, IMT-RAs show enhanced aggressive behaviors, which are possibly closely associated with their abdominopelvic origination, large tumor size, epithelioid tumoral morphology, and *RANPB2-ALK* gene rearrangement. An in-depth understanding on this entity is urgently needed to avoid misdiagnosis and provide effective treatment schedules.

Consent

Written informed consents were obtained from the patient of Case 2 and the mother of the patient of Case 1 for publication of this report and accompanying images. The copies of the written consents are available for review by the Editor-in Chief of this Journal.

Competing interests

The authors declare that they have no competing interests.

Authors' contributions

JL performed the histological, immunohistochemical and RT-PCR evaluation, literature review and drafted the manuscript. W-HY participated in histological diagnosis and immunohistochemical evaluation. KT performed FISH analysis and revised the manuscript. GH designed the study and literature review, and drafted the manuscript. Y-HH contributed to the literature review. JKCC participated in histological diagnosis and revised the manuscript. All authors read and approved the final manuscript.

References

1. Dehner LP: **Inflammatory myofibroblastic tumor: the continued definition of one type of so-called inflammatory pseudotumor.** *Am J Surg Pathol* 2004, **28:**1652–1654.

2. Coffin CM, Patel A, Perkins S, Elenitoba-Johnson KS, Perlman E, Griffin CA: **ALK1 and p80 expression and chromosomal rearrangements involving 2p23 in inflammatory myofibroblastic tumor.** *Mod Pathol* 2001, **14:**569–576.

3. Takeuchi K, Soda M, Togashi Y, Sugawara E, Hatano S, Asaka R, Okumura S, Nakagawa K, Mano H, Ishikawa Y: **Pulmonary inflammatory myofibroblastic tumor expressing a novel fusion, PPFIBP1-ALK: reappraisal of anti-ALK immunohistochemistry as a tool for novel ALK fusion identification.** *Clin Cancer Res* 2011, **17:**3341–3348.

4. Bridge JA, Kanamori M, Ma Z, Pickering D, Hill DA, Lydiatt W, Lui MY, Colleoni GW, Antonescu CR, Ladanyi M, Morris SW: **Fusion of the ALK gene to the clathrin heavy chain gene, CLTC, in inflammatory myofibroblastic tumor.** *Am J Pathol* 2001, **159:**411–415.

5. Ma Z, Hill DA, Collins MH, Morris SW, Sumegi J, Zhou M, Zuppan C, Bridge JA: **Fusion of ALK to the Ran-binding protein 2 (RANBP2) gene in inflammatory myofibroblastic tumor.** *Genes Chromosomes Cancer* 2003, **37:**98–105.

6. Yokoyama N, Hayashi N, Seki T, Panté N, Ohba T, Nishii K, Kuma K, Hayashida T, Miyata T, Aebi U: **A giant nucleopore protein that binds Ran/TC4.** *Nature* 1995, **376:**184–188.

7. Patel AS, Murphy KM, Hawkins AL, Cohen JS, Long PP, Perlman EJ, Griffin CA: **RANBP2 and CLTC are involved in ALK rearrangements in inflammatory myofibroblastic tumors.** *Cancer Genet Cytogenet* 2007, **176:**107–114.

8. Chen ST, Lee JC: **An inflammatory myofibroblastic tumor in liver with ALK and RANBP2 gene rearrangement: combination of distinct morphologic, immunohistochemical, and genetic features.** *Hum Pathol* 2008, **39:**1854–1858.

9. Butrynski JE, D'Adamo DR, Hornick JL, Dal Cin P, Antonescu CR, Jhanwar SC, Ladanyi M, Capelletti M, Rodig SJ, Ramaiya N, Kwak EL, Clark JW, Wilner KD, Christensen JG, Jänne PA, Maki RG, Demetri GD, Shapiro GI: **Crizotinib in ALK-rearranged inflammatory myofibroblastic tumor.** *N Engl J Med* 2010, **363:**1727–1733.

10. Mariño-Enríquez A, Wang WL, Roy A, Lopez-Terrada D, Lazar AJ, Fletcher CD, Coffin CM, Hornick JL: **Epithelioid inflammatory myofibroblastic sarcoma: An aggressive intra-abdominal variant of inflammatory myofibroblastic tumor with nuclear membrane or perinuclear ALK.** *Am J Surg Pathol* 2011, **35:**135–144.

11. Kozu Y, Isaka M, Ohde Y, Takeuchi K, Nakajima T: **Epithelioid inflammatory myofibroblastic sarcoma arising in the pleural cavity.** *Gen Thorac Cardiovasc Surg* 2013, **24:**.

12. Gleason BC, Hornick JL: **Inflammatory myofibroblastic tumours: where are we now?** *J Clin Pathol* 2008, **61:**428–437.

13. Coffin CM, Hornick JL, Fletcher CD: **Inflammatory myofibroblastic tumor: comparison of clinicopathologic, histologic, and immunohistochemical features including ALK expression in atypical and aggressive cases.** *Am J Surg Pathol* 2007, **31:**509–520.

14. Cook JR, Dehner LP, Collins MH, Ma Z, Morris SW, Coffin CM, Hill DA: **Anaplastic lymphoma kinase (ALK) expression in the inflammatory myofibroblastic tumor: a comparative immunohistochemical study.** *Am J Surg Pathol* 2001, **25:**1364–1371.

15. Sasaki T, Okuda K, Zheng W, Butrynski J, Capelletti M, Wang L, Gray NS, Wilner K, Christensen JG, Demetri G, Shapiro GI, Rodig SJ, Eck MJ, Jänne PA: **The neuroblastoma-associated F1174L ALK mutation causes resistance to an ALK kinase inhibitor in ALK-translocated cancers.** *Cancer Res* 2010, **70:**10038–10043.

16. Röttgers S, Gombert M, Teigler-Schlegel A, Busch K, Gamerdinger U, Slany R, Harbott J, Borkhardt A: **ALK fusion genes in children with atypical myeloproliferative leukemia.** *Leukemia* 2010, **24:**1197–1200.

17. Martorell M, Pérez-Vallés A, Gozalbo F, Garcia-Garcia JA, Gutierrez J, Gaona J: **Solitary fibrous tumor of the thigh with epithelioid features: a case report.** *Diagn Pathol* 2007, **2:**19.

18. Kim MJ, Lee SH, Youk EG, Lee S, Choi JH, Cho KJ: **Solitary myofibroma of the sigmoid colon: case report and review of the literature.** *Diagn Pathol* 2013, **8:**90.

19. Cessna MH, Zhou H, Sanger WG, Perkins SL, Tripp S, Pickering D, Daines C, Coffin CM: **Expression of ALK1 and p80 in inflammatory myofibroblastic tumor and its mesenchymal mimics: a study of 135 cases.** *Mod Pathol* 2002, **15:**931–938.

20. Uncu H, Tüzüner A: **Epithelioid leiomyosarcoma of the gastrocolic ligament.** *Acta Chir Belg* 2003, **103:**105–107.

21. Carter JM, O'Hara C, Dundas G, Gilchrist D, Collins MS, Eaton K, Judkins AR, Biegel JA, Folpe AL: **Epithelioid malignant peripheral nerve sheath tumor arising in a schwannoma, in a patient with "neuroblastoma-like" schwannomatosis and a novel germline SMARCB1 mutation.** *Am J Surg Pathol* 2012, **36:**154–160.

22. Hruban RH, Shiu MH, Senie RT, Woodruff JM: **Malignant peripheral nerve sheath tumors of the buttock and lower extremity. A study of 43 cases.** *Cancer* 1990, **66:**1253–1265.

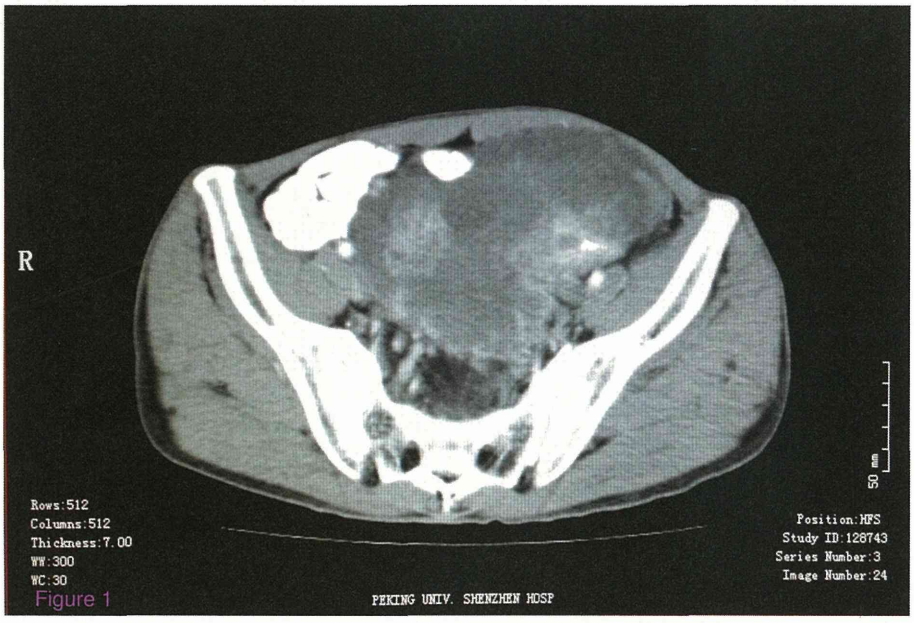
R
Rows:512
Columns:512
Thickness:7.00
WW:300
WC:30
50 mm
Position:HFS
Study ID:128743
Series Number:3
Image Number:24
PEKING UNIV. SHENZHEN HOSP
Figure 1

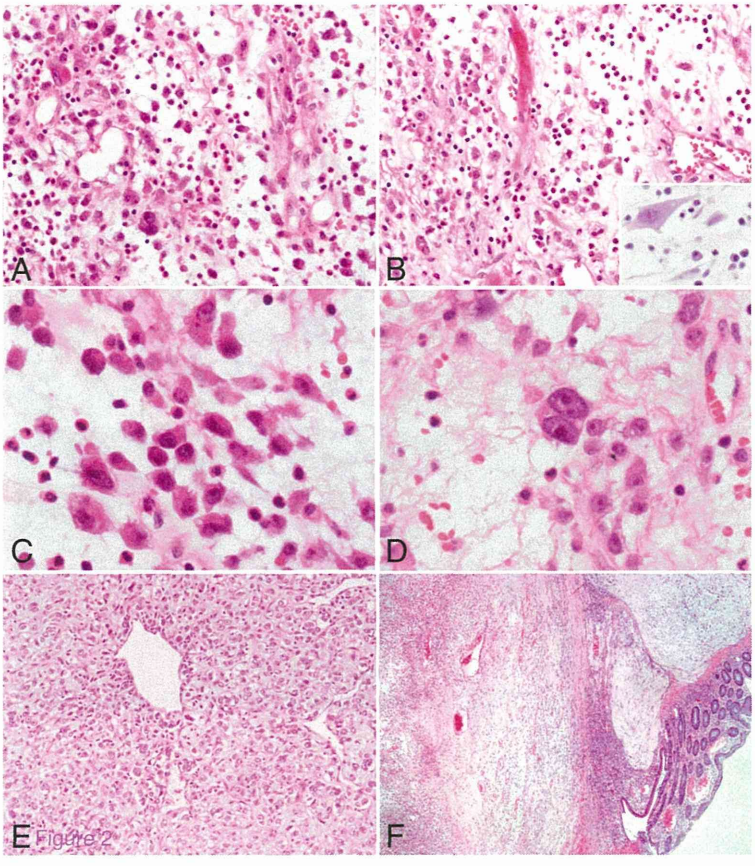

Figure 2